Bioactive Materials 15 (2022) 446–455

Contents lists available at ScienceDirect

Bioactive Materials

journal homepage: www.keaipublishing.com/en/journals/bioactive-materials

CD301b$^+$ macrophages mediate angiogenesis of calcium phosphate bioceramics by CaN/NFATc1/VEGF axis

Jiaolong Wang [a,1], Qin Zhao [a,1], Liangliang Fu [a], Shihang Zheng [a], Can Wang [a], Litian Han [a], Zijian Gong [a], Ziming Wang [a], Hua Tang [b], Yufeng Zhang [a,c,*]

[a] The State Key Laboratory Breeding Base of Basic Science of Stomatology (Hubei-MOST) and Key Laboratory of Oral Biomedicine, Ministry of Education, School & Hospital of Stomatology, Wuhan University, Wuhan, 430079, Hubei, PR China
[b] Institute of Infection and Immunity, Science and Technology Innovation Center, Shandong First Medical University & Shandong Academy of Medical Sciences, Jinan, 250000, Shandong, PR China
[c] Medical Research Institute, School of Medicine, Wuhan University, Wuhan, 430071, Hubei, PR China

ARTICLE INFO

Keywords:
Calcium phosphate ceramics
Macrophage
Angiogenesis
CD301b
Calcineurin

ABSTRACT

Calcium phosphate (CaP) bioceramics are important for tissue regeneration and immune response, yet how CaP bioceramics influence these biological processes remains unclear. Recently, the role of immune cells in biomaterial-mediated regeneration, especially macrophages, has been well concerned. CD301b$^+$ macrophages were a new subset of macrophages we have discovered, which were required for bioceramics-mediated bone regeneration. Nevertheless, the impact of CD301b$^+$ macrophages on angiogenesis, which is a vital prerequisite to bone formation is yet indistinct. Herein, we found that CD301b$^+$ macrophages were closely correlated to angiogenesis of CaP bioceramics. Additionally, depletion of CD301b$^+$ macrophages led to the failure of angiogenesis. We showed that store-operated Ca^{2+} entry and calcineurin signals regulated the VEGF expression of CD301b$^+$ macrophages via the NFATc1/VEGF axis. Inhibition of calcineurin effectively impaired angiogenesis via decreasing the infiltration of CD301b$^+$ macrophages. These findings provided a potential immunomodulatory strategy to optimize the integration of angiogenesis and bone tissue engineering scaffold materials.

1. Introduction

Biomaterials are vital components during tissue regeneration [1–4]. Previous studies have mainly focused on the effects of biomaterials on mesenchymal stem cells (MSCs), which are known for their significant functions in mediating of tissue regeneration. In recent years, biological functions of other stromal cells such as immune cells and endothelial cells, and their interactions, have become an emerging research hotspot [5–7]. Among them, immune cells can quickly respond to external stimuli, and then shape up a suitable immune niche for various stromal cells.

As innate immune cells, macrophages are the main initiators for the biomaterial-induced immune response [8]. Thus, their roles on tissue regeneration have been widely concerned [9]. Macrophages are extensively functional in the innate defense, recognition of foreign bodies, phagocytosis, regulation of inflammation, and tissue repair or fibrosis [10–13]. Actually, M1/M2 nomenclature is used to define the interferon γ (IFNγ)-activated macrophage (M1) versus the "alternative IL-4 activated" macrophage (M2) [14,15]. They are archetypal *in vitro* phenotypes, and defined according to their certain stimuli like IL-4. Besides, the considerable heterogeneity and remarkable plasticity made the various polarized phenotypes of macrophages insufficient to evaluate their regenerative effects [10,16]. To date, macrophage phenotypes with regenerative regulation, rather than inflammation modulation are still scant. Interestingly, our previous study found the regenerative regulation capacity of CD301b$^+$ macrophages during bone formation [17], which may be promising in the regeneration field. It is reported that CD301b$^+$ macrophages are widely infiltrated around the osteoinductive biomaterials [17]. They can promote osteogenic differentiation of MSCs via the IGF1R/Akt/mTOR pathway. Moreover, a few CD301b$^+$

Peer review under responsibility of KeAi Communications Co., Ltd.

* Corresponding author. The State Key Laboratory Breeding Base of Basic Science of Stomatology (Hubei-MOST) and Key Laboratory of Oral Biomedicine, Ministry of Education, School & Hospital of Stomatology, Wuhan University, Wuhan, 430079, Hubei, PR China.
E-mail address: zyf@whu.edu.cn (Y. Zhang).

[1] These authors contributed equally: Jiaolong Wang, Qin Zhao.

https://doi.org/10.1016/j.bioactmat.2022.02.004
Received 21 November 2021; Received in revised form 5 February 2022; Accepted 5 February 2022
Available online 15 February 2022

macrophages can greatly enhance the osteoinduction of biphasic calcium phosphate (BCP) bioceramics after transplantation *in vivo* [17]. On the contrary, the loss of CD301b$^+$ macrophages causes the failure of osteoinduction and thus new bone formation [17]. Hence, CD301b can be considered a potential marker for regeneration. Recently, CD301b$^+$ macrophages have been validated for their regulation capacity during skin repair and regeneration by mediating the proliferation of adipocyte precusor cells [18,19]. Transplantation with CD301b$^+$CD206$^+$ macrophages, rather than CD301b$^-$CD206$^+$ significantly facilitated skin regeneration [19]. Moreover, CD301b$^+$ and CD301b$^-$ macrophages are specific to the regenerative and fibrotic environments, respectively [20]. In particular, CD301b$^-$CD9$^+$ macrophages are highly correlated with the T helper type 17 immune response and fibrosis [20]. Therefore, we believe that CD301b$^+$ macrophages are conductive to tissue regeneration. However, many complicated and delicate biological processes are involved in bone regeneration that ultimately influence the regeneration outcome in tissue engineering. Accordingly, it is of importance but challenge to elucidate their roles in these biological responses.

Recently, the correlation between angiogenesis and osteogenesis has been well concerned as an integral and coupling processes during bone regeneration [21–25], and angiogenesis needs to be induced prior to osteogenesis [24,26,27]. Previous evidences have shown that inhibition of vascular endothelial growth factor (VEGF), an indispensable pro-angiogenic factor, would dramatically impair angiogenesis and the following bone repair and regeneration [21,22]. In addition to the well-known transportation function of circulating cells, oxygen, nutrients, and waste products, blood vessels are also supportive in bone maturation and regeneration, especially their lined endothelial cells [23,24,28,29]. It is indicated that angiogenesis of biomaterials at the early stage is beneficial to the success of bone regeneration. Therefore, it is significant and urgent to elucidate how CD301b$^+$ macrophages attribute to angiogenesis during bone regeneration.

Based on the important role of CD301b$^+$ macrophages in osteoinduction and regulation of angiogenesis, the underlying mechanism needs to be clearly elucidated. Here, BCP bioceramics were used as a standard bone substitute for their superior osteoinductivity. We confirmed CD301b$^+$ macrophages were involved in angiogenesis mediated by BCP bioceramics, and angiogenesis was mostly dependent on the expression of calcineurin (CaN). Notably, it activated the NFATc1/VEGF pathway of CD301b$^+$ macrophages, thereby promoting angiogenesis. CD301b$^+$ macrophages depletion or CaN inhibition would impair angiogenesis. Moreover, we validated the store-operated Ca^{2+} entry (SOCE) activated the CaN/NFATc1/VEGF pathway of CD301b$^+$ macrophages. This study was to clarify the mechanism of CD301b$^+$ macrophages in regulating angiogenesis, a coupling process of osteogenesis.

2. Materials and methods

2.1. Preparation and characterization of BCP bioceramics

The BCP bioceramics with a hydroxyapatite/β-tricalcium phosphate ratio of 60/40 were synthesized as previous protocols [17,30]. In brief, the BCP precursor was made by a chemical precipitation method. Then the porous BCP bioceramics were fabricated using the hydrogen peroxide foaming method, and sintered at 1100 °C for 3 h. By the way, the non-degradable CaP bioceramics were fabricated with a constant Ca/P ratio of 1.67 in the same way according to the previous protocols [17,30]. Next, grind and sieve them into a uniform size approximately 0.6 mm for further use. Scanning electron microscopy (SEM, Hitachi, Japan) were used to confirm the morphologies. The results showed that BCP bioceramics had abundant macropores (50–300 μm) and micropores (0.1–2 μm), and these pores were highly interconnected (Supplementary Fig. 1A, B).

To explore the release properties of BCP bioceramics, we immersed them into Tris-HCl solution (0.1 mol/L, pH 7.4) with a solid/liquid ratio of 0.2 g/mL at 37 °C. After 0.5, 1, 3, 7 and 14 days of immersion, 0.5 mL of immersion solution was harvested and replaced with 0.5 mL fresh Tris-HCl solution. Then, calcium ion concentration was measured by an inductively coupled plasma mass optical emission spectrometer (ICP-OES). Before quantification, the harvested solutions were diluted 10-fold.

2.2. Ethical approval and mice model

The animal experiments were conducted in accordance with the policy of Ethics Committee for Animal Research, School & Hospital of Stomatology, Wuhan University, China. The Ethics Committee for Animal Use approved it under protocol number A31/2020. The female C57BL/6 mice in around 20 g weight were maintained in specific pathogen-free condition. After 2-week adaptation to the environment, mice were utilized in the following experiments. The C57BL/6 background *Mgl2*-DTR mice (obtained from the Jackson Laboratory) were used to deplete CD301b$^+$ macrophages by diphtheria toxin (DT, Sigma, USA) administration every two days.

To establish BCP implantation model, surgery was conducted as previously described [17]. Briefly, after 150 μL intraperitoneal injection of 1% sodium pentobarbital, a deep incision about 10 mm in length was made along with the gastrocnemius muscle. Then, 2.5 mg BCP bioceramics were implanted into the incision. In addition, BCP bioceramics were also implanted into *Mgl2*-DTR mice to investigate the role of CD301b$^+$ macrophages. To uncover the underlying mechanism in angiogenesis induced by BCP bioceramics, inhibitor of CaN tacrolimus (FK506, Absin Bioscience, China) or SOCE blocker BTP2 (Absin Bioscience, China) were injected topically *in vivo* every two days. At sample harvesting time, mice were euthanized by CO_2 treatment. Then BCP-surrounding gastrocnemius muscles were acquired for further use such as histological staining and flow cytometry.

2.3. Histological staining

Fixed with 4% formaldehyde for 24 h, harvest samples were then decalcified in 10% EDTA decalcifying solution for 4 weeks and solution was refreshed each two days. Then, dehydration, embedding, and section into paraffin slices were conducted. Hematoxylin and eosin staining (H&E, Google biotechnology, China), immunohistochemistry staining (IHC, MXB biotechnologies, China) and immunofluorescence staining (IF) were carried out according to the manufacturer's protocols. For IHC and IF staining, the primary antibodies were against CD301b (eBioscience, USA), α-SMA (CST, USA), VEGF (ABclonal, China), CaN (ABclonal, China), and STIM1 (ABclonal, China). For IF staining, the anti-mouse and rabbit secondary antibodies were 594 nm red and 488 nm green fluorescent markers (Abbkine, USA). The DAPI dye (Zhongshan Biotechnology, China) was used to stain the nucleus of cells in tissue and cells. All stained sections were captured with an Olympus DP72 microscope (Olympus, Japan), and each sample was captured for 3 images of BCP bioceramics surroundings.

2.4. Extracts preparation

The extracts of BCP bioceramics were prepared according to the International Organization for Standardization (ISO 10993-5: 2009) protocol. Briefly, under a solid/liquid ratio of 0.2 g/mL, BCP bioceramics were immersed in Dulbecco's modified eagle medium (DMEM, Gibco, Thermo Fisher Scientific, USA) and incubated at 37 °C for 24 h. After centrifugation at 2500 rpm/min for 5 min and filtration through a 0.22 μm filter, the supernatants were collected carefully. Subsequently, the supernatants were supplemented with 10% fetal bovine serum (FBS, Gibco, Thermo Fisher Scientific, U.S.A). The extracts were stored at 4 °C.

2.5. Cell culture

To investigate the role of macrophages on angiogenesis induced by BCP bioceramics, bone marrow derived macrophages (BMDMs) were isolated *in vivo* according to the previous study [17]. Isolated BMDMs were cultured in DMEM containing 10% FBS and 20 ng/mL monocyte colony stimulating factor (MCSF, Peprotech, U.S.A) and culture media were refreshed every two days. Until day 7, the mature BMDMs were eligible for later experiments. Subsequently, BCP extracts were used to replace the original culture media to incubate BMDMs in the presence or absence of 1 mM FK506 (Absin Bioscience, China) or 500 nM BTP2 (Absin Bioscience, China). Next, BMDMs were collected for future RNA and protein extraction, and the supernatants were centrifuged at 2500 rpm/min for 5 min and frozen at −80 °C used as conditioned media for further culture of human umbilical vein endothelial cells (HUVECs, Mixed donors, Lonza). To carry out vessel tube formation *in vitro*, HUEVCs were maintained and expanded in DMEM containing 10% FBS at 37 °C and 5% CO_2 humid atmosphere.

2.6. Flow cytometry

Samples were dissected and digested with RPMI-1640 containing collagenase II (2 μg/mL, Sigma-Aldrich, USA) for 1 h at 37 °C. The remaining tissues were filtered through 70-μm cell strainers, washed with PBS for 3 times, and then centrifuged at 2500 rpm, 5 min. After discarding the supernatant, enriched single-cell suspension was incubated with an antibody panel for 30 min, 4 °C. The antibodies used were as follows, CD45-phycoerythrin (PE, 1:400, Biolegend, U.S.A), CD11b-Blue (Biolegend, 1:200, U.S.A), F4/80-PE-cyanine7 (Cy7, 1:400, Biolegend, U.S.A), CD301b-PerCP (Biolegend, 1:400, U.S.A), CD9-allophycocyanin (APC, 1:400, Biolegend, U.S.A), NFATc1-PE (1:200, Biolegend, U.S.A). Cells were examined by a BD Biosciences LSR Fortessa flow cytometer (BD Biosciences, USA), and data was analyzed by FlowJo software (Treestar, U.S.A).

2.7. Protein extraction and Western blotting

About 100 μL RIPA buffer containing protease inhibitor and 1% phosphatase inhibitors was used to lyse the cells and collected into the pre-cooled tube, followed by ultrasonic treatment on ice. Each sample was quantified and normalized by BCA kit (Thermo Fisher Scientific, USA). After mixed with 5X loading buffer, the protein mixture was heated for 10 min at 95 °C. Then, successive steps of separation by SDS-PAGE gelatin, transfer to nitrocellulose, soaking into 5% fat-free milk and incubation with primary and secondary antibodies (BioSharp, China) were carried out. The primary antibodies were against STIM1 (ABclonal, China), CaN (ABclonal, China), VEGF (ABclonal, China), NFATc1 (ABclonal, China) and GAPDH (ABclonal, China). At last, the results were visualized by WesternBright ECL HRP Substrate Kit (Advansta, U.S.A).

2.8. RNA extraction, RNA-seq and RT-qPCR

For RNA-seq analysis, tissues around BCP biocramics were harvested, rinsed by PBS for three times and frozen quickly under liquid nitrogen atmosphere. Then, the total RNA was extracted with TRIzol (TAKARA, Japan) and followed by sequencing with Illumina Platform. For realtime-quantitative polymerase chain reaction (RT-qPCR) analysis, cell samples were collected and treated with TRIzol reagent to extract their total RNA in accordance with the manufacturer's protocol. After cDNA synthesis, RT-qPCR analysis was conducted with PrimeScript RT-PCR Kit (TAKARA, Japan). The forward and reversed primer sequences of the target genes were listed in Supplementary Table 1.

2.9. Tube formation in vitro

To evaluate the angiogenic ability of HUEVCs after stimulation with the conditioned media *in vitro*, a tube formation assay was conducted. Briefly, growth factor reduced basement membrane matrix (Corning, U.S.A) was used to coat 96-well plate (50 μL/well, Nest, USA) and incubated at 37 °C and 5% CO_2 for 30 min. When growth factor reduced basement membrane matrix was solidified, HUVECs were then seeded in 96-well plate at 25,000 cells/well in either DMEM medium (positive control) or harvested conditioned media. Then HUVECs were incubated in a humid atmosphere of 5% CO_2 at 37 °C. After 4 h, photos were captured with a light microscope (Nikon, Japan) under a bright field to record cells and developed tubules. Angiogenesis-related parameters including meshes, master junctions and branches were examined by ImageJ software using the Angiogenesis Analyzer plugin (NIH, Bethesda, MD, USA).

2.10. Measurement of intracellular calcium ion concentration

The intracellular calcium ions of BMDMs were evaluated after stimulation with BCP bioceramics for 12 h. BMDMs were incubated with 5 μM calcein-AM (Dojindo, Kumamoto Prefecture, Japan) according to the manufacturer's guidelines. The visualization of the intracellular Ca^{2+} was captured with a laser scanning confocal microscope (InSIGHT Plus-IQ, Meridian, USA) at an excitation wavelength of 488 nm. Also, the cells were loaded with 4 μM fluo-3 (Beyotime Institute of Biotechnology, China), which was dissolved in dimethyl sulphoxide (1:1000) in Dulbecco's Phosphate Buffered Saline (DPBS) for 30 min in the dark at 37 °C. Then, the fluorescence intensity was measured by a BD Biosciences LSR Fortessa flow cytometer (BD Biosciences, USA), and data was analyzed by FlowJo software (Treestar, U.S.A).

2.11. Statistical analysis

Statistical analyses were conducted by the GraphPad Prism software (v6.0, GraphPad, USA). The differences among each group were evaluated through two-way ANOVA or students' t-test. Significant statistical differences were considered when $^{*}P < 0.05$, $^{**}P < 0.01$, $^{***}P < 0.001$.

3. Results

3.1. $CD301b^{+}$ macrophages are required for angiogenesis during osteoinduction

We first implanted BCP bioceramics into the gastrocnemius muscle *in vivo*. Four weeks later, the histological staining results showed the formation of new bone around BCP bioceramics, suggesting the excellent osteoinductive ability BCP bioceramics (Suppl. Fig. 2). We detected multiple time points after implantation to confirm angiogenesis. H&E staining showed that new blood vessels were formed in the BCP-implanted sites (Suppl. Fig. 3). To evaluate the infiltration of $CD301b^{+}$ macrophages, samples at 7 and 14 days were examined by IHC staining and flow cytometry. On day 7 after implantation, $CD301b^{+}$ macrophages around BCP bioceramcis ranked about 50%, which remarkably increased and reached 70.6% on day 14 (Fig. 1A and B). Additionally, α-SMA, a crucial marker of angiogenesis, was strongly expressed around BCP bioceramics, which was more pronounced on day 14 (Fig. 1C). Interestingly, the increase positive expression of α-SMA was temporally corresponded with infiltration of $CD301b^{+}$ macrophages (Fig. 1C). To further examine the correlation between $CD301b^{+}$ macrophages and angiogenesis *in vivo*, macrophage galactose-type C-type lectin 2 (Mgl2, encoding the CD301b protein) -DTR mice (*Mgl2*-DTR) were used, in which $CD301b^{+}$ macrophages were depleted [17–19]. Loss of $CD301b^{+}$ macrophages in *Mgl2*-DTR mice was confirmed by IF staining (Suppl. Fig. 4). After DT treatment every two days following BCP bioceramics implantation, α-SMA expression was significantly

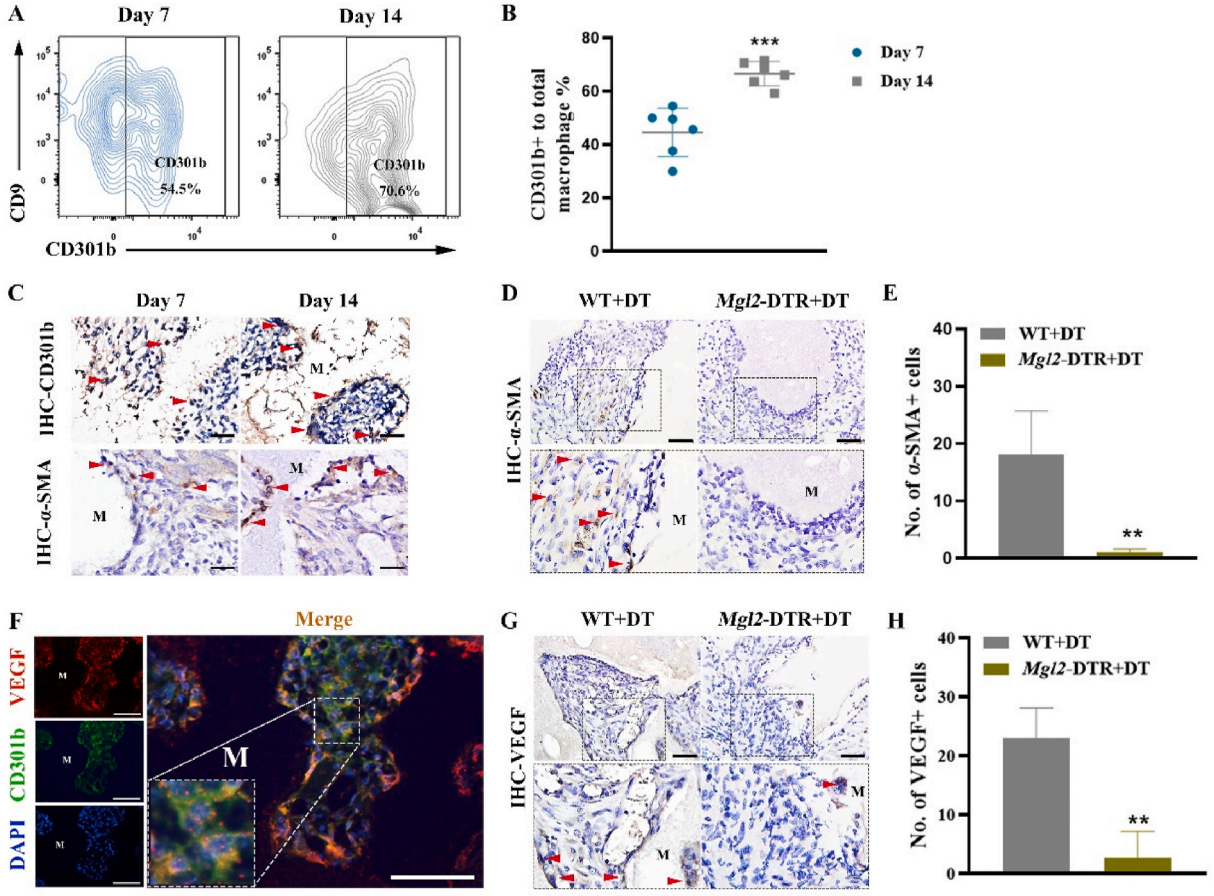

Fig. 1. (A) Flow cytometry analysis of CD301b$^+$ macrophages in the tissues surrounding BCP bioceramics at 14 days after implantation. (B) Semiquantification of gating strategy cells in (A). ***$P < 0.001$. (C) IHC staining of regenerative macrophages subsets CD301b and α-SMA after BCP bioceramics implantation at 7 and 14 days (the red arrow showed the positive cells; M, material). Scale bar = 200 μm. (D) IHC staining of α-SMA in BCP implant areas after CD301b$^+$ macrophages depletion at 14 days (the red arrow showed the positive cells; M, material). Scale bar = 100 μm. (E) Semiquantification of positively stained cells in (D). **$P < 0.01$. (F) IF staining of VEGF (red), CD301b (green) and nuclei (blue) at 14 days after BCP bioceramics implantation *in vivo*. (Scale bar = 100 μm). (G) IHC staining of VEGF in BCP implant areas after CD301b$^+$ macrophages depletion at 14 days (the red arrow showed the positive cells; M, material). Scale bar = 100 μm. (H) Semiquantification of positively stained cells in (G). **$P < 0.01$. (For interpretation of the references to colour in this figure legend, the reader is referred to the Web version of this article.)

downregulated in *Mgl2*-DTR mice than that of control mice on day 14, suggesting the angiogenesis impairment (Fig. 1D and E). In addition, IF staining showed that CD301b was barely co-localized with α-SMA (Suppl. Fig. 5). It is suggested that DT treatment would not directly downregulate α-SMA.

VEGF is not only essential for angiogenesis, but also for a tight coupling between angiogenesis and osteogenesis during bone repair and regeneration [5,31]. Thus, we detected the expression of VEGF by IF staining. Distribution and colocalization of VEGF and CD301b around BCP bioceramics on day 14 were observed (Fig. 1F). Besides, a continual loss of CD301b$^+$ macrophages resulted in VEGF deficiency around BCP bioceramics (Fig. 1G and H). These data suggested that CD301b$^+$ macrophages essentially upregulated VEGF, which were required for angiogenesis during osteoinduction.

3.2. BCP bioceramics activates pathways related to calmodulin-binding protein CaN and SOCE

To figure out the molecular mechanism underlying angiogenesis, RNA-seq analysis after BCP and non-degradable CaP bioceramics implantation *in vivo* was performed. A total of 142 differentially expressed genes (DEG) were detected between BCP and non-degradable CaP bioceramics, involving 111 genes upregulated genes and 31 downregulated ones (Suppl. Fig. 6). After the enrichment analysis of RNA-seq results, DEG were found to be enriched into gene sets related to the calmodulin-binding pathway (Fig. 2A). It is indicated that BCP bioceramics created an environment with high levels of calmodulin-binding proteins. Furthermore, expression levels of several common and critical calmodulin-binding proteins in macrophages like CaMKII, CaMKK2, CaN after stimulation with BCP bioceramics were detected by RT-qPCR. Only CaN and ORAI1 were significantly upregulated (Fig. 2B). Additionally, VEGF was upregulated after BCP stimulation (Suppl. Fig. 8). BCP bioceramics were found to continually release Ca^{2+} ions (Suppl. Fig. 5), and chelation of Ca^{2+} ions by EDTA prevented upregulation of CaN and VEGF induced by BCP bioceramics (Suppl. Fig. 9). Based on the core function of ORAI1 in SOCE, we further determined expression levels of key proteins in the SOCE pathway signaling, including ORAI2, STIM1, STIM2, PLC-γ, NFATc1, and NFATc2. Most of them were upregulated by BCP bioceramics (Fig. 2C). These data showed that BCP bioceramics activated pathways related to calmodulin-binding protein CaN and SOCE.

3.3. The CaN signaling pathway and SOCE control the pro-angiogenesis potential of CD301b$^+$ macrophages

The regulatory role of SOCE in key proteins involved in the Ca^{2+}-dependent signaling molecules, including CaN, and CaN activated the nuclear factor of activated T cells (NFAT) has been validated [32]

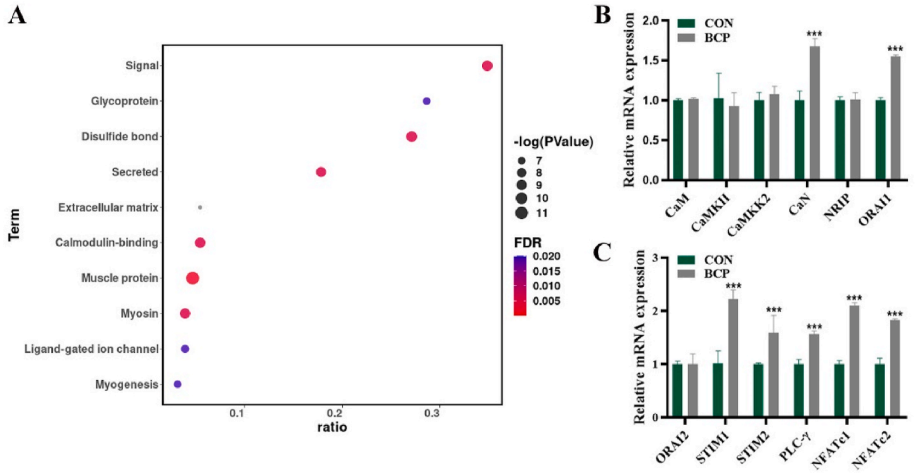

Fig. 2. (A) Enrichment analysis of differentially expressed genes after BCP bioceramics implantation. (B) Relative mRNA expression of calmodulin-binding proteins after extracts of BCP bioceramics stimulation. (C) Relative mRNA expression of SOCE proteins after extracts of BCP bioceramics stimulation.

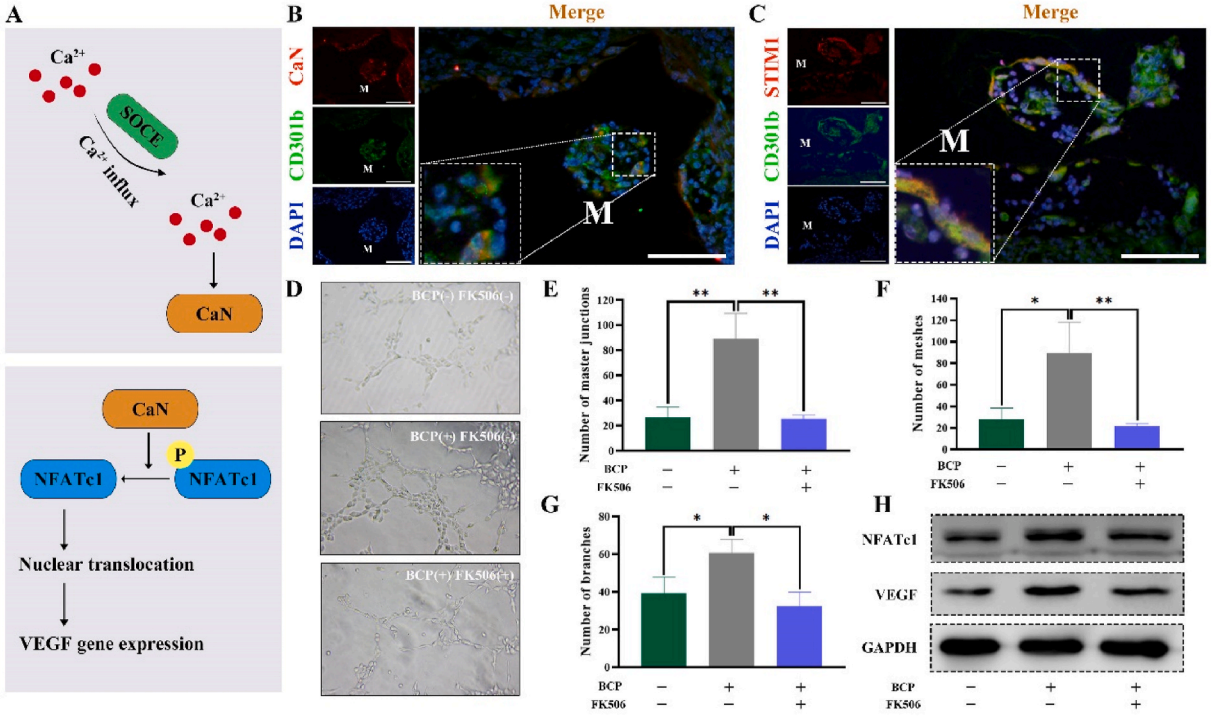

Fig. 3. (A) Schematic illustration of CaN and SOCE pathways. (B) IF staining of CaN (red), CD301b (green) and nuclei (blue) at 14 days after BCP bioceramics implantation *in vivo* (M, material). Scale bar = 100 μm. (C) IF staining of STIM1 (red), CD301b (green) and nuclei (blue) at 14 days after BCP bioceramics implantation *in vivo* (M, material). Scale bar = 100 μm. (D) An *in vitro* tube formation assay in Matrigel of HUEVCs incubated with conditioned media from three groups. (E–G) Quantification of the network characteristics in (D). $^{**}P < 0.01$, $^{***}P < 0.001$. (H) Activation of NFATc1/VEGF pathway after stimulation from of three groups presented by Western blotting. (For interpretation of the references to colour in this figure legend, the reader is referred to the Web version of this article.)

(Fig. 3A). Activated NFAT contributes to promote angiogenesis by inducing the positive expression of VEGF [33] (Fig. 3A). To determine the involvement of the CaN signaling pathway and SOCE in the pro-angiogenesis potential of $CD301b^{+}$ macrophages, expression levels of CaN and STIM1 were detected by IF staining. Both CaN and STIM1 were co-expressed with CD301b surrounding BCP bioceramics (Fig. 3B and C). Interestingly, an *in vitro* tube formation assay of HUEVCs showed that number of master junctions and meshes were going at about three times in the group of macrophages-conditioned media pretreated with BCP extracts. This group also showed more branches in the organized networks (Fig. 3D, E, F, G). By contrast, application of tacrolimus (FK506), an inhibitor targeted CaN reversed it, indicating that CaN was responsible for angiogenesis (Fig. 3D, E, F, G). Furthermore, protein levels of NFATc1 and VEGF were unregulated after BCP stimulation, which were reversed by inhibiting CaN (Fig. 3H). These data were consistent with the tube formation findings. Notably, the median fluorescence intensity of NFATc1 in macrophages around BCP bioceramics were higher than that in macrophages around non-degradable CaP bioceramics. VEGF in macrophages showed the similar trend. These data demonstrated that BCP bioceramics upregulated NFATc1 and VEGF expressions of the surrounding macrophages (Suppl. Fig. 10).

After treatment with the SOCE inhibitor BTP2, the protein level of CaN was downregulated (Fig. 4A). Similar results were obtained in protein levels of NFATc1 and VEGF as well, suggesting that CaN was

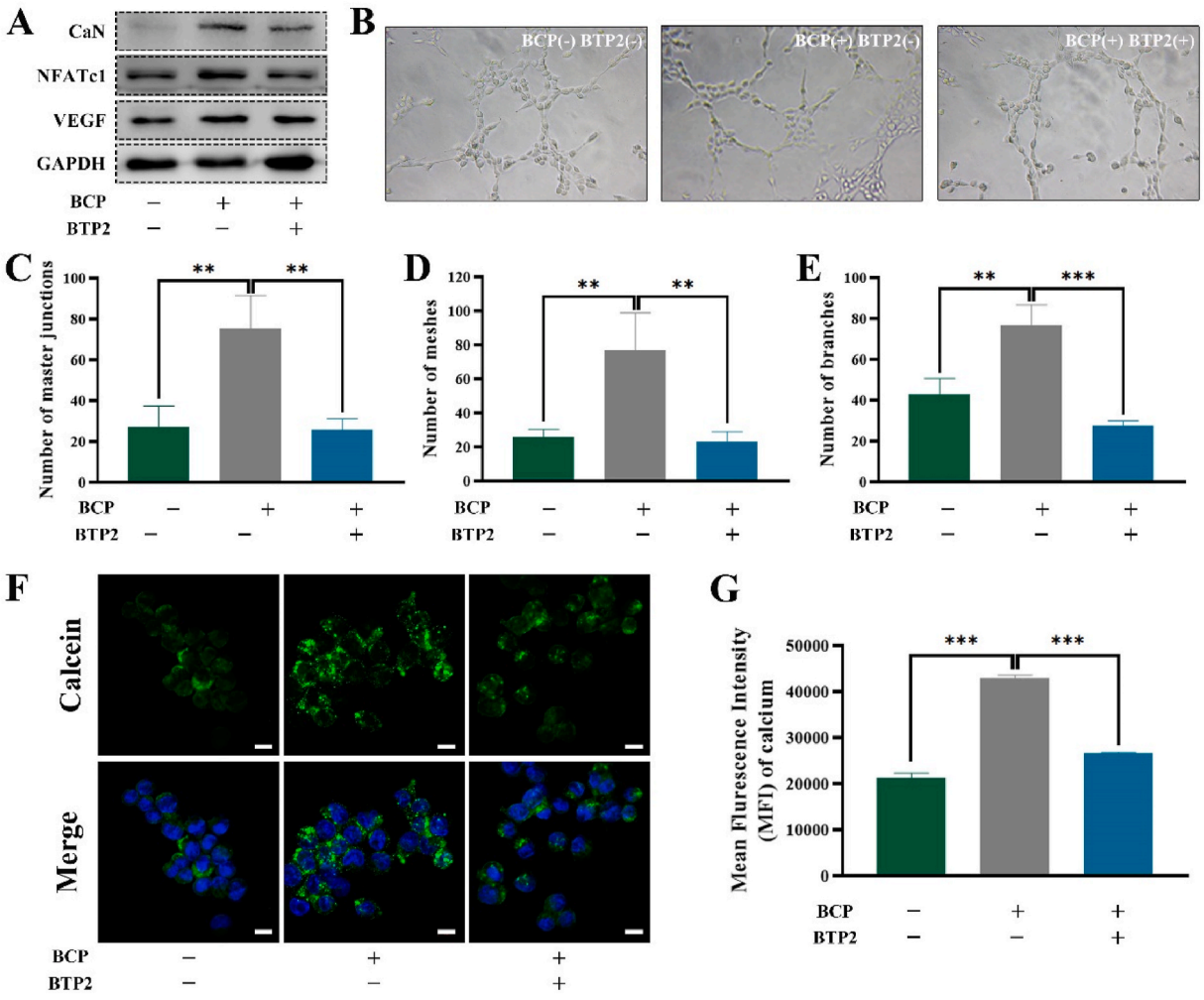

Fig. 4. (A) Activation of NFATc1/VEGF pathway after stimulation from of three groups presented by Western blotting. (B) An *in vitro* tube formation assay in Matrigel of HUEVCs incubated with conditioned media from three groups. (C–E) Quantification of the network characteristics in (B). $^{*}P < 0.05$, $^{**}P < 0.01$. (F) Confocal microscopy images of intracellular Ca^{2+} concentration after treatment with BCP and BTP2. Scale bar = 10 μm. (G) Quantification of intracellular Ca^{2+} concentration detected by flow cytometry.

responsible for the biological function of SOCE (Fig. 4A). Besides, the SOCE inhibitor BTP2 prevented BCP bioceramics from playing a positive role in tube formation *in vitro*. The levels of master junctions, branches and nodes dropped to the levels in the unstimulated HUEVCs group (Fig. 4B, C, D, E). An *in vivo* study confirmed that SOCE was required for the positive expression of VEGF around BCP bioceramics (Suppl. Fig. 11). Additionally, the concentration of free cytosolic Ca^{2+} significantly increased after stimulation with BCP bioceramics, while the application of BTP2 blocked the entry of free Ca^{2+} into macrophages as verified by fluorescence staining and flow cytometry (Fig. 4F and G). Since CaN activity was regulated by free cytosolic Ca^{2+}, defective Ca^{2+} influx induced by the SOCE inhibitor BTP2 was responsible for the impaired angiogenesis potential.

3.4. CaN signaling pathway is necessary for angiogenesis

To confirm the contribution of CaN signaling to angiogenesis, CaN inhibitor FK506 was administrated every two days after implantation. Importantly, a substantial decrease in the expression of VEGF around BCP bioceramics was observed (Fig. 5A and B), and α-SMA was barely expressed around the BCP bioceramics (Fig. 5C and D). Taken together, these data implicated the necessity of the CaN signaling pathway for angiogenesis.

3.5. CaN signaling pathway regulates the infiltration of CD301b^{+} macrophages around BCP bioceramics

We next determined the role of the CaN signaling pathway in promoting angiogenesis via regulating macrophages. However, IHC staining and flow cytometry did not obtain a significant change in the number of the infiltrated macrophages around BCP bioceramics (Fig. 6A, B, C). Due to the great heterogeneity of macrophages, we hypothesized that the subset CD301b^{+} macrophages were affected by the CaN signaling pathway. Interestingly, the infiltration of CD301b^{+} macrophages reduced from 84.8% to 58.8% after CaN inhibition on day 14 (Fig. 6D, E, F). These data indicated that CaN signaling pathway regulated the infiltration of CD301b^{+} macrophages during osteoinduction induced by BCP bioceramics.

4. Discussion

Immune cells are critical for bone regeneration induced by osteoinductive biomaterials, especially macrophages. It is reported that loss of macrophages impairs tissue regeneration [34]. Macrophages were highly heterogeneous and plastic, which are responsive to diverse cues and environments. M1/M2 polarization has attracted extensive attention because of their inflammatory regulation capacity. Osteoinductive bioceramics have been found to regulate macrophage polarization [30,

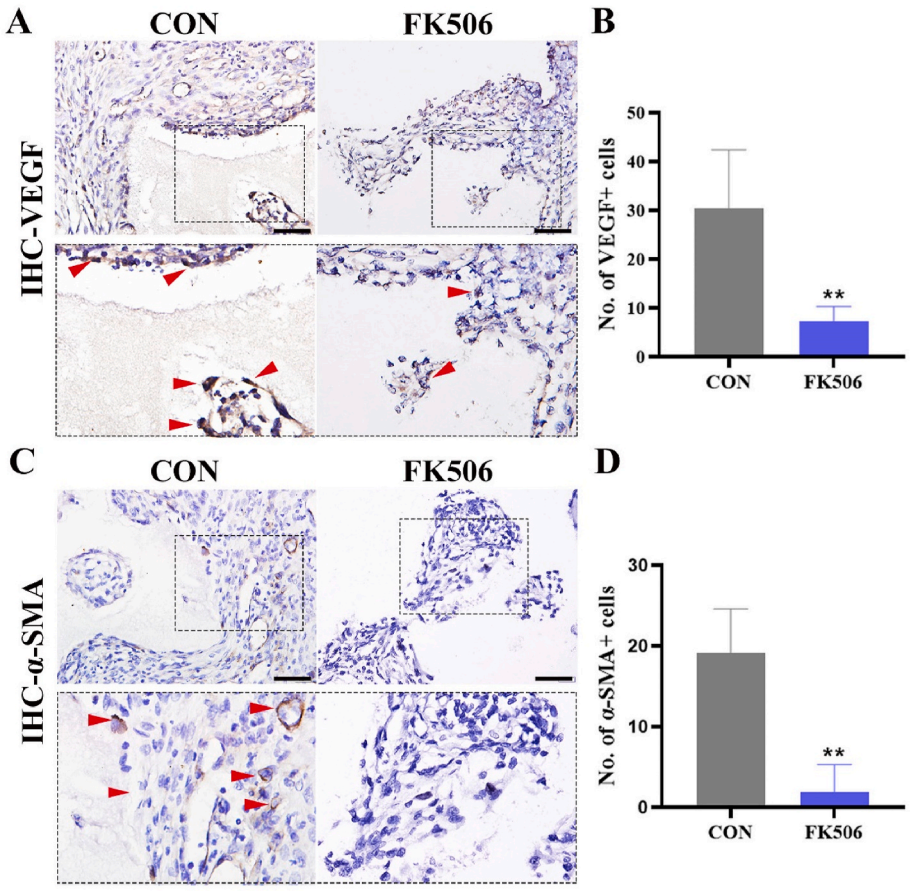

Fig. 5. (A) IHC staining of VEGF in BCP implant areas after treatment with FK506 at day 14 (the red arrow showed the positive cells; M, material). Scale bar = 100 μm. (B) Semiquantification of positively stained cells in (A). $^{**}P < 0.01$. (C) IHC staining of α-SMA in BCP implant areas after treatment with FK506 (the red arrow showed the positive cells; M, material). Scale bar = 100 μm. (B) Semiquantification of positively stained cells in (C). $^{**}P < 0.01$. (For interpretation of the references to colour in this figure legend, the reader is referred to the Web version of this article.)

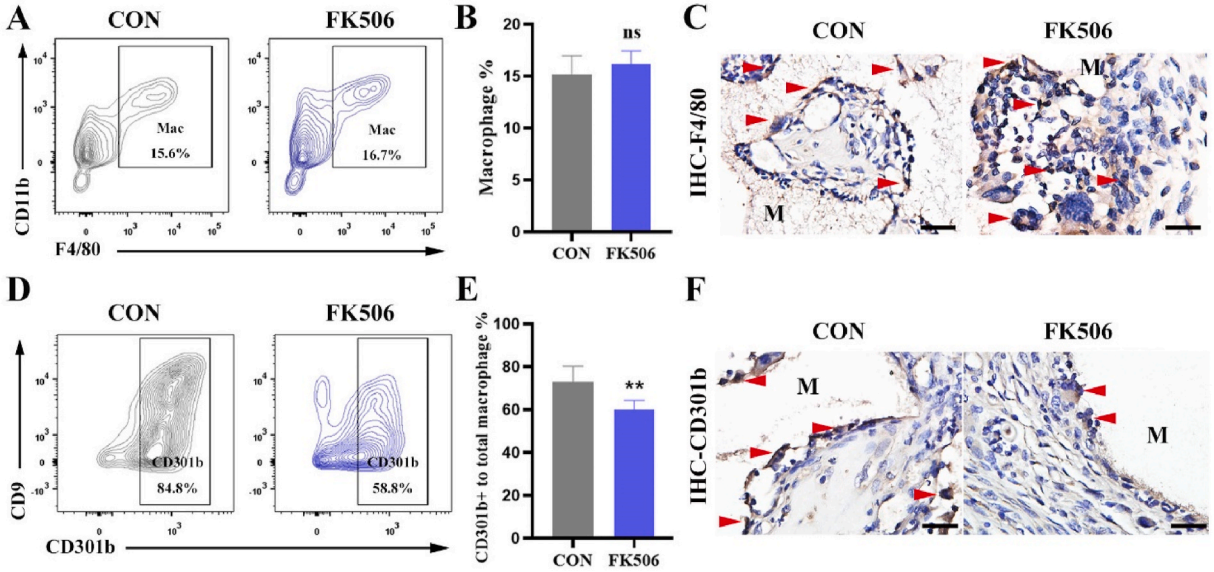

Fig. 6. (A) Flow cytometry analysis of total macrophages in the tissues surrounding BCP bioceramics at 14 days after implantation. (B) Semiquantification of gating strategy cells in (A), ns means no significance. (C) IHC staining of macrophages (F4/80) around BCP bioceramics at day 14 (the red arrow showed the positive cells; M, material). Scale bar = 100 μm. (D) Flow cytometry analysis of $CD301b^{+}$ macrophages in the tissues surrounding BCP bioceramics at 14 days after implantation. (E) Semiquantification of gating strategy cells in (D). $^{**}P < 0.01$. (F) IHC staining of regenerative macrophages subsets (CD301b) around BCP bioceramics at day 14 (the red arrow showed the positive cells; M, material). Scale bar = 100 μm. (For interpretation of the references to colour in this figure legend, the reader is referred to the Web version of this article.)

35–37]. However, whether M1 or M2 is beneficial to angiogenesis remains controversial [38]. Some studies have demonstrated that M1 induce endothelial cells to germinate and M2 promote vascular anastomosis during the angiogenesis process [39]. Actually, M1/M2 macrophages are *in vitro* phenotypes, which defined according to certain bioactive factors [14,15]. However, implantation of bare biomaterials without any bioactive factors is supposed to affect macrophages phenotypes *in vivo* as well. M1/M2 phenotypes rarely overlap with those found in physiological conditions, as indicated by recent single-cell RNA sequencing and mass cytometry [20,40,41]. Therefore, M1 and M2 macrophages have not been clearly analyzed for their potential application in bone regeneration. Unlike polarization, CD301b$^+$ macrophages are the subsets closely correlated with tissue regeneration. Previous *in vivo* studies have demonstrated that CD301b$^+$ macrophages activate the proliferation of adipocyte precursors through insulin-like growth factor 1 and platelet-derived growth factor C, thus contributing to skin repair and formation [18]. Sommerfeld et al. demonstrated that CD301b$^+$ macrophages held some M1 macrophage subset and parts of M2 macrophage subset [20]. CD301b$^+$ macrophages expressed high levels of multiple cytokines like IL1 and Arg1, considering as typical M1 and M2 cytokines, respectively. Canonical polarization markers are distributed across CD301b$^+$ and CD301b$^-$ macrophages clusters. CD86 and CD206 did not discriminate between phenotypically distinct subsets, while CD301b marker separates macrophages specific to the regenerative microenvironment [20]. Previous studies have well elucidated the close correlation between CD301b$^+$ macrophages and bone regeneration induced by BCP bioceramics [17]. In this study, we further confirmed that CD301b$^+$ macrophages were required for angiogenesis, and refined the understanding of the regulatory role of regenerative macrophages on angiogenesis.

As a crucial process for bone formation, angiogenesis is essential for bone repair and regeneration [23,24,42]. CaP bioceramics used to be analyzed for its potential on osteogenesis-related processes, yet how it affects angiogenesis is rarely concerned [23]. Bone healing is a complex process consisting of several overlapping stages, in which many cellular and molecular processes are involved in. Complications like delayed healings and non-union are common due to failure of vascular reconstruction rather than lack of osteogenic potential [23,43]. In practice, the bone substitute at the implantation site is more demand for vascularization than that of the normal bone defect healing [23]. Without the prerequisite blood supply, osteogenesis is difficult to proceed [23]. Notably, the coupling link between angiogenic and osteogenic cells and signals emphasizes the importance of these interactions [23,24,27]. Bone tissue engineering usually focused on osteoconduction, osteoinduction, and osteogenesis. In contrast, the diamond concept with more clinically relevant has highlighted the vascular environment [44]. Therefore, to elucidate the role and mechanism of CaP bioceramics in angiogenesis is meaningful for developing bone substitutes. α-SMA is widely expressed in the capillary pericytes, which can be regarded as a marker of newly-formed capillaries [45,46]. Here we found that α-SMA expressed in the CaP-implanted sites. Loss of CD301b$^+$ macrophages resulted in the non-detectable α-SMA around CaP bioceramics. Previous studies have suggested that CaP bioceramics can promote blood vessel formation [47–49], which is consistent with our findings.

In this study, we found that CD301b$^+$ macrophage served as the responder immediately to bioceramics implantation, which was of importance in promoting angiogenesis induced by CaP bioceramics. It upregulated VEGF, a factor essential for angiogenesis to foster angiogenesis. In fact, angiogenesis existed around BCP at the late stage even without the involvement of CD301b$^+$ macrophages (data not shown), which was not the focus of this article. The inflammatory response immediately occurred following the implantation of bioceramics [50]. More importantly, loss of CD301b$^+$ macrophages inhibited angiogenesis at the early stage around BCP bioceramics. Moreover, bioceramics enhanced the secretion of angiogenesis-related factors by osteoblasts [51]. These cues suggest that the role of CD301b$^+$ macrophages was mainly manifested in the early stage, and other cells like osteoblasts were functional in the late stage. Numerous studies have explored the way to improve angiogenic responses by various strategies, including delivering of VEGF, doping with strontium ions, and prevascularization [50,52,53]. These efforts underscored the importance of early vascularization. Therefore, the effect of CD301b$^+$ macrophages on early vascularization is a meaningful topic to be addressed.

Many studies have demonstrated that Ca^{2+} ions released from CaP bioceramics contribute to modulate the biological behavior of macrophages [54–56]. Continuous release of Ca^{2+} ions from CaP bioceramics activates the Wnt/β-catenin pathway in macrophages through the calcium-sensitive receptor CaSR, thus promoting the M2 macrophages [56]. Another study also shows that Ca^{2+} ions are involved in the regulatory effect of CaP bioceraics on macrophage polarization via upregulating IκBα [37]. Ca^{2+} ion concentration varies in CaP bioceramics, leading to distinct macrophage phenotypes [37,56]. Actually, our study focused on the similar topic with previous findings, but a new perspective was proposed. In addition, it is recognized that Ca^{2+} ions drove angiogenesis by recruiting multiple Ca^{2+} ions-sensitive decorders in response to pro-angiogenic cues [57]. Consistently, we found that BCP bioceramics significantly upregulated the Ca^{2+} ion-dependent signaling. They activated the SOCE and CaN, which promoted angiogenesis via mediating the infiltration of CD301b$^+$ macrophages and expression level of VEGF. Compared with those around non-degradable CaP bioceramics, both NFATc1 and VEGF in macrophages around BCP bioceramics showed more robust expressions. It verified the role of Ca^{2+} ions released from BCP bioceramics. In fact, both calcium cations and phosphate anions were released from CaP bioceramics once degraded [23]. However, less was known about the role phosphate ions in physiological functions than that of Ca^{2+} ions [53]. It is reported that phosphate ions regulate the differentiation and growth of skeleton cells via the IGF1 and ERK1/2 pathways [58]. Besides, they inhibit osteoclast differentiation and bone resorption via RANK-ligand and its receptor signaling [54,59]. The relationship between phosphate ions and angiogenesis needs to be elucidated in the future [23].

Local administration of CaN inhibitor mainly inhibited CaN of CD301b$^+$ macrophages for the fact that CD301b and CaN were widely expressed and highly overlapped around CaP bioceramics, although we did not specifically interfere with CaN of macrophages. Recently, CaN has been found to participate in many biological behaviors through the Ca^{2+}-dependent signal transduction pathways [60]. In lung endothelial cells, CaN/NFATc1 signal axis is able to promote lung repair by regulating the expression of thromboplastin-1 [61]. It controls myelin clearance in Schwann cells by regulating autophagy, which is very important for axon regeneration and remyelination after peripheral nerve injury [62]. CaN is also essential to promote skeletal muscle regeneration through regulating expression levels of muscle synthesis genes MyoD, Myf5, and Myogenin [63,64]. CaN is also involved in controlling T cell proliferation and subsequent adaptive immune response by upregulating glycolysis and oxidative phosphorylation [32]. These findings underscored the vital role of CaN in a variety of different regenerative environments. Our study elucidated the molecular mechanisms of CaN in promoting angiogenesis induced by the osteoinductive CaP bioceramics. It may provide a potential target for regulating angiogenesis and ultimately osteogenesis.

5. Conclusion

In our study, we highlighted the important role of CD301b$^+$ macrophages in angiogenesis mediated by osteoinductive bioceramics. BCP bioceramics released Ca^{2+}, and activated CD301b$^+$ macrophages. They promoted angiogenesis through SOCE and CaN/NFATc1/VEGF pathway. Furthermore, CaN inhibitor blocked the infiltration of CD301b$^+$ macrophages. Finally, because the full integration of angiogenesis with tissue engineering strategies would facilitate tissue regeneration, our identification of a role of CD301b$^+$ macrophages in

angiogenesis of BCP bioceramics may have broad implications for the future design of biomaterial-oriented tissue engineering.

Data availability

The data that support the findings of this study are present in the paper and/or the Supplementary Materials. Additional data related to this paper can be acquired from the authors upon reasonable request.

CRediT authorship contribution statement

Jiaolong Wang: Conceptualization, Supervision, Investigation, Formal analysis, Visualization, Validation, Writing – original draft, Writing – review & editing. **Qin Zhao:** Conceptualization, Methodology, Supervision, Resources, Formal analysis, Writing – review & editing. **Liangliang Fu:** Investigation, Formal analysis, Visualization, Validation. **Shihang Zheng:** Formal analysis, Investigation. **Can Wang:** Investigation. **Litian Han:** Software, Formal analysis. **Zijian Gong:** Investigation. **Ziming Wang:** Investigation. **Hua Tang:** Resources. **Yufeng Zhang:** Conceptualization, Supervision, Funding acquisition, Writing – review & editing.

Declaration of competing interest

The authors declare that they have no known competing financial interests or personal relationships that could have appeared to influence the work reported in this paper.

Acknowledgements

This work was supported by the National Natural Science Foundation of China (82025011 and 82100975); the China National Postdoctoral Program for Innovative Talents (BX2021227); the Young Elite Scientist Support Program by CSA (2020PYRC001); and the Fundamental Research Funds for the Central Universities (2042021kf0181 and 2042020kf0204).

Appendix A. Supplementary data

Supplementary data to this article can be found online at https://doi.org/10.1016/j.bioactmat.2022.02.004.

References

[1] S. Pina, J.M. Oliveira, R.L. Reis, Natural-based nanocomposites for bone tissue engineering and regenerative medicine: a review, Adv. Mater. 27 (7) (2015) 1143–1169, https://doi.org/10.1002/adma.201403354.
[2] S. Bose, N. Sarkar, Natural medicinal compounds in bone tissue engineering, Trends Biotechnol. 38 (4) (2020) 404–417, https://doi.org/10.1016/j.tibtech.2019.11.005.
[3] A. Ho-Shui-Ling, J. Bolander, L.E. Rustom, A.W. Johnson, F.P. Luyten, C. Picart, Bone regeneration strategies: engineered scaffolds, bioactive molecules and stem cells current stage and future perspectives, Biomaterials 180 (2018) 143–162, https://doi.org/10.1016/j.biomaterials.2018.07.017.
[4] J.J. Li, M. Ebied, J. Xu, H. Zreiqat, Current approaches to bone tissue engineering: the interface between biology and engineering, Adv Healthc Mater 7 (6) (2018), e1701061, https://doi.org/10.1002/adhm.201701061.
[5] Y. Niu, Z. Wang, Y. Shi, L. Dong, C. Wang, Modulating macrophage activities to promote endogenous bone regeneration: biological mechanisms and engineering approaches, Bioact Mater 6 (1) (2021) 244–261, https://doi.org/10.1016/j.bioactmat.2020.08.012.
[6] L. Chung, D.R. Maestas Jr., F. Housseau, J.H. Elisseeff, Key players in the immune response to biomaterial scaffolds for regenerative medicine, Adv. Drug Deliv. Rev. 114 (2017) 184–192, https://doi.org/10.1016/j.addr.2017.07.006.
[7] J. Lee, H. Byun, S.K. Madhurakkat Perikamana, S. Lee, H. Shin, Current advances in immunomodulatory biomaterials for bone regeneration, Adv Healthc Mater 8 (4) (2019), e1801106, https://doi.org/10.1002/adhm.201801106.
[8] P. Zhou, D. Xia, Z. Ni, T. Ou, Y. Wang, H. Zhang, L. Mao, K. Lin, S. Xu, J. Liu, Calcium silicate bioactive ceramics induce osteogenesis through oncostatin M, Bioact Mater 6 (3) (2021) 810–822, https://doi.org/10.1016/j.bioactmat.2020.09.018.
[9] S. Franz, S. Rammelt, D. Scharnweber, J.C. Simon, Immune responses to implants - a review of the implications for the design of immunomodulatory biomaterials, Biomaterials 32 (28) (2011) 6692–6709, https://doi.org/10.1016/j.biomaterials.2011.05.078.
[10] R.J. Miron, D.D. Bosshardt, OsteoMacs: key players around bone biomaterials, Biomaterials 82 (2016) 1–19, https://doi.org/10.1016/j.biomaterials.2015.12.017.
[11] P. Zhang, Q. Zhao, M. Shi, C. Yin, Z. Zhao, K. Shen, Y. Qiu, Y. Xiao, Y. Zhao, X. Yang, Y. Zhang, Fe3O4@TiO2-Laden neutrophils activate innate immunity via photosensitive reactive oxygen species release, Nano Lett. 20 (1) (2020) 261–271, https://doi.org/10.1021/acs.nanolett.9b03777.
[12] T.A. Wynn, K.M. Vannella, Macrophages in tissue repair, regeneration, and fibrosis, Immunity 44 (3) (2016) 450–462, https://doi.org/10.1016/j.immuni.2016.02.015.
[13] Q. Zhao, J. Wang, C. Yin, P. Zhang, J. Zhang, M. Shi, K. Shen, Y. Xiao, Y. Zhao, X. Yang, Y. Zhang, Near-infrared light-sensitive nano neuro-immune blocker capsule relieves pain and enhances the innate immune response for necrotizing infection, Nano Lett. 19 (9) (2019) 5904–5914, https://doi.org/10.1021/acs.nanolett.9b01459.
[14] A. Mantovani, A. Sica, S. Sozzani, P. Allavena, A. Vecchi, M. Locati, The chemokine system in diverse forms of macrophage activation and polarization, Trends Immunol. 25 (12) (2004) 677–686, https://doi.org/10.1016/j.it.2004.09.015.
[15] C.D. Mills, K. Kincaid, J.M. Alt, M.J. Heilman, A.M. Hill, M-1/M-2 macrophages and the Th1/Th2 paradigm, J. Immunol. 164 (12) (2000) 6166–6173, https://doi.org/10.4049/jimmunol.164.12.6166.
[16] P.J. Murray, Macrophage polarization, Annu. Rev. Physiol. 79 (1) (2017) 541–566, https://doi.org/10.1146/annurev-physiol-022516-034339.
[17] J. Wang, Q. Zhao, S. Zheng, W. Jinyang, L. Fu, C. Wang, Z. Zhao, Y. Zhang, Break monopoly of polarization: CD301b+ macrophages play positive roles in osteoinduction of calcium phosphate ceramics, Appl. Mater. Today 24 (2021) 101111, https://doi.org/10.1016/j.apmt.2021.101111.
[18] B.A. Shook, R.R. Wasko, G.C. Rivera-Gonzalez, E. Salazar-Gatzimas, F. López-Giráldez, B.C. Dash, A.R. Muñoz-Rojas, K.D. Aultman, R.K. Zwick, V. Lei, J. L. Arbiser, K. Miller-Jensen, D.A. Clark, H.C. Hsia, V. Horsley, Myofibroblast proliferation and heterogeneity are supported by macrophages during skin repair, Science 362 (6417) (2018), https://doi.org/10.1126/science.aar2971.
[19] B. Shook, E. Xiao, Y. Kumamoto, A. Iwasaki, V. Horsley, CD301b+ macrophages are essential for effective skin wound healing, J. Invest. Dermatol. 136 (9) (2016) 1885–1891, https://doi.org/10.1016/j.jid.2016.05.107.
[20] S.D. Sommerfeld, C. Cherry, R.M. Schwab, L. Chung, D.R. Maestas Jr., P. Laffont, J. E. Stein, A. Tam, S. Ganguly, F. Housseau, J.M. Taube, D.M. Pardoll, P. Cahan, J. H. Elisseeff, Interleukin-36γ-producing macrophages drive IL-17-mediated fibrosis, Sci Immunol 4 (40) (2019), https://doi.org/10.1126/sciimmunol.aax4783.
[21] J. Street, M. Bao, L. deGuzman, S. Bunting, F.V. Peale Jr., N. Ferrara, H. Steinmetz, J. Hoeffel, J.L. Cleland, A. Daugherty, N. van Bruggen, H.P. Redmond, R.A. Carano, E.H. Filvaroff, Vascular endothelial growth factor stimulates bone repair by promoting angiogenesis and bone turnover, Proc. Natl. Acad. Sci. U. S. A. 99 (15) (2002) 9656–9661, https://doi.org/10.1073/pnas.152324099.
[22] K.A. Jacobsen, Z.S. Al-Aql, C. Wan, J.L. Fitch, S.N. Stapleton, Z.D. Mason, R. M. Cole, S.R. Gilbert, T.L. Clemens, E.F. Morgan, T.A. Einhorn, L.C. Gerstenfeld, Bone formation during distraction osteogenesis is dependent on both VEGFR1 and VEGFR2 signaling, J. Bone Miner. Res. 23 (5) (2008) 596–609, https://doi.org/10.1359/jbmr.080103.
[23] A. Malhotra, P. Habibovic, Calcium phosphates and angiogenesis: implications and advances for bone regeneration, Trends Biotechnol. 34 (12) (2016) 983–992, https://doi.org/10.1016/j.tibtech.2016.07.005.
[24] A.P. Kusumbe, S.K. Ramasamy, R.H. Adams, Coupling of angiogenesis and osteogenesis by a specific vessel subtype in bone, Nature 507 (7492) (2014) 323–328, https://doi.org/10.1038/nature13145.
[25] M. Wang, Y. Yu, K. Dai, Z. Ma, Y. Liu, J. Wang, C. Liu, Improved osteogenesis and angiogenesis of magnesium-doped calcium phosphate cement via macrophage immunomodulation, Biomater Sci 4 (11) (2016) 1574–1583, https://doi.org/10.1039/c6bm00290k.
[26] E.C. Novosel, C. Kleinhans, P.J. Kluger, Vascularization is the key challenge in tissue engineering, Adv. Drug Deliv. Rev. 63 (4) (2011) 300–311, https://doi.org/10.1016/j.addr.2011.03.004.
[27] S.K. Ramasamy, A.P. Kusumbe, L. Wang, R.H. Adams, Endothelial Notch activity promotes angiogenesis and osteogenesis in bone, Nature 507 (7492) (2014) 376–380, https://doi.org/10.1038/nature13146.
[28] E.C. Novosel, C. Kleinhans, P.J. Kluger, Vascularization is the key challenge in tissue engineering, Adv. Drug Deliv. Rev. 63 (4–5) (2011) 300–311, https://doi.org/10.1016/j.addr.2011.03.004.
[29] J. Rouwkema, A. Khademhosseini, Vascularization and angiogenesis in tissue engineering: beyond creating static networks, Trends Biotechnol. 34 (9) (2016) 733–745, https://doi.org/10.1016/j.tibtech.2016.03.002.
[30] X. Chen, M. Wang, F. Chen, J. Wang, X. Li, J. Liang, Y. Fan, Y. Xiao, X. Zhang, Correlations between macrophage polarization and osteoinduction of porous calcium phosphate ceramics, Acta Biomater. 103 (2020) 318–332, https://doi.org/10.1016/j.actbio.2019.12.019.
[31] K. Hu, B.R. Olsen, Osteoblast-derived VEGF regulates osteoblast differentiation and bone formation during bone repair, J. Clin. Invest. 126 (2) (2016) 509–526, https://doi.org/10.1172/jci82585.
[32] M. Vaeth, M. Maus, S. Klein-Hessling, E. Freinkman, J. Yang, M. Eckstein, S. Cameron, S.E. Turvey, E. Serfling, F. Berberich-Siebelt, R. Possemato, S. Feske, Store-operated Ca(2+) entry controls clonal expansion of T cells through metabolic

reprogramming, Immunity 47 (4) (2017) 664–679, https://doi.org/10.1016/j.immuni.2017.09.003, e6.
[33] M.R. Müller, A. Rao, NFAT, immunity and cancer: a transcription factor comes of age, Nat. Rev. Immunol. 10 (9) (2010) 645–656, https://doi.org/10.1038/nri2818.
[34] Q. Zhao, M. Shi, C. Yin, Z. Zhao, J. Zhang, J. Wang, K. Shen, L. Zhang, H. Tang, Y. Xiao, Y. Zhang, Dual-wavelength photosensitive nano-in-micro scaffold regulates innate and adaptive immune responses for osteogenesis, Nano-Micro Lett. 13 (1) (2020) 28, https://doi.org/10.1007/s40820-020-00540-z.
[35] O.R. Mahon, D.C. Browe, T. Gonzalez-Fernandez, P. Pitacco, I.T. Whelan, S. Von Euw, C. Hobbs, V. Nicolosi, K.T. Cunningham, K.H.G. Mills, D.J. Kelly, A. Dunne, Nano-particle mediated M2 macrophage polarization enhances bone formation and MSC osteogenesis in an IL-10 dependent manner, Biomaterials 239 (2020) 119833, https://doi.org/10.1016/j.biomaterials.2020.119833.
[36] Z. Chen, S. Ni, S. Han, R. Crawford, S. Lu, F. Wei, J. Chang, C. Wu, Y. Xiao, Nanoporous microstructures mediate osteogenesis by modulating the osteo-immune response of macrophages, Nanoscale 9 (2) (2017) 706–718, https://doi.org/10.1039/c6nr06421c.
[37] Z. Chen, C. Wu, W. Gu, T. Klein, R. Crawford, Y. Xiao, Osteogenic differentiation of bone marrow MSCs by β-tricalcium phosphate stimulating macrophages via BMP2 signalling pathway, Biomaterials 35 (5) (2014) 1507–1518, https://doi.org/10.1016/j.biomaterials.2013.11.014.
[38] J. Kitajewski, Wnts heal by restraining angiogenesis, Blood 121 (13) (2013) 2381–2382, https://doi.org/10.1182/blood-2013-01-479063.
[39] K.L. Spiller, R.R. Anfang, K.J. Spiller, J. Ng, K.R. Nakazawa, J.W. Daulton, G. Vunjak-Novakovic, The role of macrophage phenotype in vascularization of tissue engineering scaffolds, Biomaterials 35 (15) (2014) 4477–4488, https://doi.org/10.1016/j.biomaterials.2014.02.012.
[40] M.M. Gubin, E. Esaulova, J.P. Ward, O.N. Malkova, D. Runci, P. Wong, T. Noguchi, C.D. Arthur, W. Meng, E. Alspach, R.F.V. Medrano, C. Fronick, M. Fehlings, E. W. Newell, R.S. Fulton, K.C.F. Sheehan, S.T. Oh, R.D. Schreiber, M.N. Artyomov, High-dimensional analysis delineates myeloid and lymphoid compartment remodeling during successful immune-checkpoint cancer therapy, Cell 175 (4) (2018) 1014–1030, https://doi.org/10.1016/j.cell.2018.09.030, e19.
[41] A.C. Villani, R. Satija, G. Reynolds, S. Sarkizova, K. Shekhar, J. Fletcher, M. Griesbeck, A. Butler, S. Zheng, S. Lazo, L. Jardine, D. Dixon, E. Stephenson, E. Nilsson, I. Grundberg, D. McDonald, A. Filby, W. Li, P.L. De Jager, O. Rozenblatt-Rosen, A.A. Lane, M. Haniffa, A. Regev, N. Hacohen, Single-cell RNA-seq reveals new types of human blood dendritic cells, monocytes, and progenitors, Science 356 (6335) (2017), https://doi.org/10.1126/science.aah4573.
[42] H.H. Xu, P. Wang, L. Wang, C. Bao, Q. Chen, M.D. Weir, L.C. Chow, L. Zhao, X. Zhou, M.A. Reynolds, Calcium phosphate cements for bone engineering and their biological properties, Bone Res 5 (2017) 17056, https://doi.org/10.1038/boneres.2017.56.
[43] K. Schmidt-Bleek, H. Schell, N. Schulz, P. Hoff, C. Perka, F. Buttgereit, H.-D. Volk, J. Lienau, G.N. Duda, Inflammatory phase of bone healing initiates the regenerative healing cascade, Cell Tissue Res. 347 (3) (2012) 567–573, https://doi.org/10.1007/s00441-011-1205-7.
[44] P.V. Giannoudis, T.A. Einhorn, G. Schmidmaier, D. Marsh, The diamond concept – open questions, Injury 39 (2008) S5–S8, https://doi.org/10.1016/S0020-1383(08)70010-X.
[45] Q. Wu, S. Xu, X. Wang, B. Jia, Y. Han, Y. Zhuang, Y. Sun, Z. Sun, Y. Guo, H. Kou, C. Ning, K. Dai, Complementary and synergistic effects on osteogenic and angiogenic properties of copper-incorporated silicocarnotite bioceramic: in vitro and in vivo studies, Biomaterials 268 (2021) 120553, https://doi.org/10.1016/j.biomaterials.2020.120553.
[46] L. Alarcon-Martinez, S. Yilmaz-Ozcan, M. Yemisci, J. Schallek, K. Kılıç, A. Can, A. Di Polo, T. Dalkara, Capillary pericytes express α-smooth muscle actin, which requires prevention of filamentous-actin depolymerization for detection, Elife 7 (2018), https://doi.org/10.7554/eLife.34861.
[47] Y. Chen, J. Wang, X.D. Zhu, Z.R. Tang, X. Yang, Y.F. Tan, Y.J. Fan, X.D. Zhang, Enhanced effect of β-tricalcium phosphate phase on neovascularization of porous calcium phosphate ceramics: in vitro and in vivo evidence, Acta Biomater. 11 (2015) 435–448, https://doi.org/10.1016/j.actbio.2014.09.028.
[48] W.E.G. Müller, M. Ackermann, B. Al-Nawas, L.A.R. Righesso, R. Muñoz-Espí, E. Tolba, M. Neufurth, H.C. Schröder, X. Wang, Amplified morphogenetic and bone forming activity of amorphous versus crystalline calcium phosphate/polyphosphate, Acta Biomater. 118 (2020) 233–247, https://doi.org/10.1016/j.actbio.2020.10.023.
[49] U. Ritz, H. Götz, A. Baranowski, F. Heid, P.M. Rommens, A. Hofmann, Influence of different calcium phosphate ceramics on growth and differentiation of cells in osteoblast-endothelial co-cultures, J. Biomed. Mater. Res. B Appl. Biomater. 105 (7) (2017) 1950–1962, https://doi.org/10.1002/jbm.b.33728.
[50] F. Zhao, B. Lei, X. Li, Y. Mo, R. Wang, D. Chen, X. Chen, Promoting in vivo early angiogenesis with sub-micrometer strontium-contained bioactive microspheres through modulating macrophage phenotypes, Biomaterials 178 (2018) 36–47, https://doi.org/10.1016/j.biomaterials.2018.06.004.
[51] Z. Gu, H. Xie, L. Li, X. Zhang, F. Liu, X. Yu, Application of strontium-doped calcium polyphosphate scaffold on angiogenesis for bone tissue engineering, J. Mater. Sci. Mater. Med. 24 (5) (2013) 1251–1260, https://doi.org/10.1007/s10856-013-4891-8.
[52] F. Wei, G. Liu, Y. Guo, R. Crawford, Z. Chen, Y. Xiao, Blood prefabricated hydroxyapatite/tricalcium phosphate induces ectopic vascularized bone formation via modulating the osteoimmune environment, Biomater Sci 6 (8) (2018) 2156–2171, https://doi.org/10.1039/c8bm00287h.
[53] P. Habibovic, J.E. Barralet, Bioinorganics and biomaterials: bone repair, Acta Biomater. 7 (8) (2011) 3013–3026, https://doi.org/10.1016/j.actbio.2011.03.027.
[54] J. Jeong, J.H. Kim, J.H. Shim, N.S. Hwang, C.Y. Heo, Bioactive calcium phosphate materials and applications in bone regeneration, Biomater. Res. 23 (2019) 4, https://doi.org/10.1186/s40824-018-0149-3.
[55] Z. Changchun, L. Xiangfeng, C. Junqiu, F. Hongsong, Z. Xingdong, Bioactive Ceramics and Metals for Regenerative Engineering, Regenerative Engineering, CRC Press2018.
[56] J. Zhang, Q. Wu, C. Yin, X. Jia, Z. Zhao, X. Zhang, G. Yuan, H. Hu, Q. Zhao, Sustained calcium ion release from bioceramics promotes CaSR-mediated M2 macrophage polarization for osteoinduction, J. Leukoc. Biol. (2021), https://doi.org/10.1002/jlb.3ma0321-739r.
[57] F. Moccia, S. Negri, M. Shekha, P. Faris, G. Guerra, Endothelial Ca(2+) signaling, angiogenesis and vasculogenesis: just what it takes to make a blood vessel, Int. J. Mol. Sci. 20 (16) (2019), https://doi.org/10.3390/ijms20163962.
[58] M. Julien, S. Khoshniat, A. Lacreusette, M. Gatius, A. Bozec, E.F. Wagner, Y. Wittrant, M. Masson, P. Weiss, L. Beck, D. Magne, J. Guicheux, Phosphate-dependent regulation of MGP in osteoblasts: role of ERK1/2 and Fra-1, J. Bone Miner. Res. 24 (11) (2009) 1856–1868, https://doi.org/10.1359/jbmr.090508.
[59] A. Mozar, N. Haren, M. Chasseraud, L. Louvet, C. Mazière, A. Wattel, R. Mentaverri, P. Morlière, S. Kamel, M. Brazier, J.C. Mazière, Z.A. Massy, High extracellular inorganic phosphate concentration inhibits RANK-RANKL signaling in osteoclast-like cells, J. Cell. Physiol. 215 (1) (2008) 47–54, https://doi.org/10.1002/jcp.21283.
[60] F. Rusnak, P. Mertz, Calcineurin: form and function, Physiol. Rev. 80 (4) (2000) 1483–1521, https://doi.org/10.1152/physrev.2000.80.4.1483.
[61] J.H. Lee, D.H. Bhang, A. Beede, T.L. Huang, B.R. Stripp, K.D. Bloch, A.J. Wagers, Y. H. Tseng, S. Ryeom, C.F. Kim, Lung stem cell differentiation in mice directed by endothelial cells via a BMP4-NFATc1-thrombospondin-1 axis, Cell 156 (3) (2014) 440–455, https://doi.org/10.1016/j.cell.2013.12.039.
[62] C.B. Reed, L.R. Frick, A. Weaver, M. Sidoli, E. Schlant, M.L. Feltri, L. Wrabetz, Deletion of calcineurin in Schwann cells does not affect developmental myelination, but reduces autophagy and delays myelin clearance after peripheral nerve injury, J. Neurosci. 40 (32) (2020) 6165–6176, https://doi.org/10.1523/jneurosci.0951-20.2020.
[63] N. Stupka, B.J. Michell, B.E. Kemp, G.S. Lynch, Differential calcineurin signalling activity and regeneration efficacy in diaphragm and limb muscles of dystrophic mdx mice, Neuromuscul. Disord. 16 (5) (2006) 337–346, https://doi.org/10.1016/j.nmd.2006.03.003.
[64] M.K. Tu, J.B. Levin, A.M. Hamilton, L.N. Borodinsky, Calcium signaling in skeletal muscle development, maintenance and regeneration, Cell Calcium 59 (2–3) (2016) 91–97, https://doi.org/10.1016/j.ceca.2016.02.005.